

Letter of Intent for J-PARC 50 GeV Synchrotron

Modification of baryon structure in nuclear matter studied from beta-decay rate of a Λ hypernucleus

Kento Kamada^a, Manami Fujita^b, Hirokazu Tamura^{a,b}

^a *Department of Physics, Tohoku University*

^b *Advances Science Research Center, Japan Atomic Energy Agency*

abstract

Although the EMC effect indicates that structure of baryons in nuclear matter is modified from that in the free space, no clear evidence for baryon modification in matter has been found in low energy nuclear phenomena and detailed mechanism of the modification is not understood yet. In order to challenge this problem, we propose to measure the beta-decay rate of a Λ hyperon in a nucleus. The hyperon beta-decay rate can be significantly reduced in a nucleus, if an u (and d) quark wave functions is more spread due to meson field in a nucleus than an s quark wave function, which reduces overlap between u and s quark wavefunctions in the beta-decay. The quark-meson-coupling (QMC) model predicts reduction of the Λ 's beta-decay rate by 20% at maximum.

We will measure the beta-decay rate of ${}^5_{\Lambda}\text{He}$ in 4.5% accuracy. In large nuclei, neutron beta-decay rate is greatly suppressed due to nuclear many-body effects and meson-exchange-current effects. To avoid such “ g_A quenching” effects we chose ${}^5_{\Lambda}\text{He}$ hypernucleus.

The experiment will be carried out at the K1.1 beam line by employing the ${}^6\text{Li}(\pi^+, K^+){}^5_{\Lambda}\text{He}+p$ reaction with the SKS spectrometer. The branching ratio of the beta-decay will be determined in 4 % accuracy by measuring the energy spectrum of the beta-decay electrons with a 4π calorimeter made of BGO crystal. The weak decay lifetime of ${}^5_{\Lambda}\text{He}$ will be also determined in 2% accuracy by directly measuring the time difference between the beam pion and the weak decay particles (protons from nonmesonic decay). The weak decay of ${}^5_{\Lambda}\text{He}$ was previously studied in KEK E462 using the same reaction and almost the same apparatus. Thus, the yield of the proposed experiment is reliably estimated based on the E462 results.

Through simulation studies we have found that the huge backgrounds from the main weak decay modes can be efficiently removed and the experiment is feasible in a realistic beam time and conditions. Namely, by using 3×10^7 π^+ /spill, the beta-decay rate is estimated to be measured within 4.5% accuracy in ~ 1500 hours of beam time (1400 hours for the branching ratio measurement and 120 hours for the lifetime measurement).

After detailed design of the detectors and further simulations, we are planning to submit a full proposal to the next PAC meeting.

1 Motivation

Low energy nuclear phenomena have been described in terms of structureless nucleons, although the nucleons are known to have substructure made of quarks and gluons together with meson clouds, which distribute over the nucleon radius of the same order of magnitude as the inter-nucleon distance in a nucleus. Thus, it is natural to conjecture that the nucleon structure is modified in a nucleus from that in the free space. Actually, the EMC effect indicates that the momentum distribution of quarks in nucleons in a nucleus is significantly changed from those in the free space [1]. Recently, it was found that the main part of the EMC effect ($0.35 < x_B < 0.7$), where the deep inelastic cross section is reduced from that in the free space, is strongly correlated with the nucleon-nucleon short-range correlation scale factors [2]. Although this observation provides a clue to unravel the EMC effect, the mechanism of the EMC effect has not become clear yet.

Various discussions have been made on how and why the nucleon structure is modified in a nucleus, but there has been no clear experimental evidence for the modification except for the EMC effect. In other words, the modification has not been established in low energy nuclear phenomena. It is partly because complicated nuclear many-body effects do not allow one to separately extract possible effects of the nucleon modification.

We propose a measurement of the beta-decay rate of a Λ hyperon in a nucleus. It has been discussed that a nucleon in the nucleus may be swelled; the distribution of u and d quarks are possibly spread due to the meson field. Here, as schematically shown in Fig. 1, the distribution of an s quark in the hyperon is expected to stay unchanged because the coupling of s quarks in the baryon with the meson field is considered to be much smaller than that of u and d quarks. When beta-decay of the hyperon takes place in the nucleus, the overlap between the unchanged s quark wave function and the spread u quark wave function is expected to be reduced. This structure change can be observed as a reduction of the axial charge g_A of the hyperon in the nucleus.

This effect was estimated by the quark meson coupling (QMC) model [3]. It incorporates interactions between the scalar and vector mesons in the nucleus and the confined u and d quarks in the baryon, and the structure of the baryon is self-consistently determined by the interactions, where the coupling parameters are fixed from nuclear saturation density and energy. According to Ref. [3], the axial coupling constant of Λ (g_A^Λ) is predicted to be reduced by $\sim 10\%$ in the nuclear saturation density. This calculation suggests a significant (up to 20%) reduction of the beta-decay rate of a Λ hyperon in the nucleus.

The g_A value from the neutron beta-decay is known to be quenched in a nucleus as shown in Fig. 2 [4]. Such g_A quenching phenomena are considered to arise from nuclear many-body effects as well as hadronic effects such as meson exchange current [5]. Possible effects from nucleon modification due to change of quark distribution are, even if they exist, probably hindered by these nuclear and hadronic effects. The g_A quenching effect is measured to be large (30-40%) for heavy nuclei, but is $\sim 5\%$ for light ($A \leq 4$) nuclei [4], as shown in Fig. 2. Thus, by using a light (s -shell) hypernucleus, we can minimize these effects and expect to observe a clear evidence for the baryon modification. In addition, ab initio calculations for nuclear beta-decay are available for light nuclei. For example, the ${}^6\text{He}$ beta-decay rate was reproduced within 2% accuracy [6]. We expect that similar ab initio calculations can be performed and all the many-body effects and the meson exchange current effects in the g_A value can be precisely estimated. Therefore, we propose to measure the g_A value of the ${}^5_\Lambda\text{He}$ hypernucleus, which has a mass number small enough but a significantly large density.

Table 1: Total and partial weak decay rates of ${}^5_\Lambda\text{He}$ hypernucleus shown in the unit of the free Λ decay rate, Γ_Λ .

Experiment/Theory	$\Gamma_{tot}/\Gamma_\Lambda$	$\Gamma_{\pi^-}/\Gamma_\Lambda$	$\Gamma_{\pi^0}/\Gamma_\Lambda$	$\Gamma_{nm}/\Gamma_\Lambda$
Exp. (K^-, π^-), BNL [7]	1.03 ± 0.08	0.44 ± 0.11	0.18 ± 0.20	0.41 ± 0.14
Exp. (π^+, K^+), KEK [8, 9]	0.947 ± 0.038	0.340 ± 0.016	0.201 ± 0.011	0.406 ± 0.020
Theor. [10] (YNG)		0.393	0.215	
Theor. [11]		0.386	0.196	
Theor. [12]	0.966			0.358
Theor. [13] (NSC97f)			0.317	
Theor. [14]			0.43	

2 Principle of the experiment

We propose a precise determination of the beta-decay rate Γ_β of a Λ hyperon in the ${}^5_\Lambda\text{He}$ hypernucleus. We measure the weak decay lifetime τ and the beta-decay branching ratio B_β of ${}^5_\Lambda\text{He}$ and derive the beta-decay rate $\Gamma_\beta = B_\beta/\tau$ with a statistical error less than 4% and a systematic error much lower than that. Provided that the beta-decay of a Λ in ${}^5_\Lambda\text{He}$ does not excite the 0^+ α core, the ${}^5_\Lambda\text{He}$ beta-decay has the same structure as the Λ beta-decay in the free space. Namely, we can assume that

$$\Gamma_\beta \propto (g_V^\Lambda)^2 \left| \int 1|^2 + (g_A^\Lambda)^2 \left| \int \sigma|^2 = (g_V^\Lambda)^2 + 3(g_A^\Lambda)^2 \sim 1 + 1.55$$

because $g_V^\Lambda = 1$ and $g_A^\Lambda = -0.718 \pm 0.015$ for a Λ in the free space, and a change of Γ_β in nuclear matter is attributed to a change of g_A^Λ since g_V^Λ is (almost) unchanged [3]. Since a fraction (1.55/2.55) of Γ_β comes from the axial current, Γ_β is expected to be reduced by $(1.55/2.55) \times 2 \times 10\% = 12\%$ if g_A^Λ is reduced by 10%. The proposed experiment aims at measurement of Γ_β in 4.5% accuracy, which corresponds to the accuracy of g_A of $4.5 \times (2.55/1.55)/2 = 3.7\%$.

The main difficulty of this experiment comes from a very small branching ratio of the beta-decay of Λ , $(8.32 \pm 0.14) \times 10^{-4}$ in free space as shown in Fig. 3, and possible huge backgrounds coming from the other decay modes, the mesonic weak decay ($\Lambda \rightarrow p\pi^-$ and $n\pi^0$) and the non-mesonic weak decay ($\Lambda N \rightarrow NN$). Their branching ratios were measured at BNL and then KEK as summarized in Table 1, where they are shown in terms of the decay rates in the unit of the free Λ 's decay rate. As shown in the table, these values are theoretically reproduced well.

In order to clearly identify the beta-decay event, we employ a calorimeter covering almost 4π sr surrounding the target to select one-cluster shower events and measure the electron energy. We also install plastic counters and Lucite Cherenkov counters close to the target to identify one-charged-particle event with fast velocity.

It is noted that the decay rate for $\Lambda \rightarrow n\gamma$, whose branching ratio in the free space is 1.75×10^{-3} , may be also changed in a nucleus due to possible change of the u , d quark distribution, although theoretical calculation of this process is difficult. This decay mode has a larger branching ratio than the beta-decay and makes a peak in the γ -ray energy spectrum. Thus we can also measure its decay rate.

2.1 Production reaction of the hypernuclei

${}^5_{\Lambda}\text{He}$ hypernuclei will be produced via the ${}^6\text{Li}(\pi^+, K^+)$ reaction with a ${}^6\text{Li}$ metal target. The ground state of the ${}^6_{\Lambda}\text{Li}$ hypernucleus produced by the ${}^6\text{Li}(\pi^+, K^+)$ reaction decays via proton emission to ${}^5_{\Lambda}\text{He}$ (only the ground state is bound in ${}^5_{\Lambda}\text{He}$).

As shown in Fig. 4, the structure of ${}^6_{\Lambda}\text{Li}$ hypernucleus was studied via the (K^-, π^-) reaction [15], which revealed three structures: the unbound ground state with the $n(p_{3/2}^{-1})\Lambda(s_{1/2})$ configuration, the ~ 8 MeV excited states with the $n(p_{3/2}^{-1})\Lambda(p_{3/2})$ configuration, and the 18 MeV excited state with $n(s_{1/2}^{-1})\Lambda(s_{1/2})$ configuration. The second and third structures are so-called ‘‘substitutional states’’ which are populated by $\Delta L = 0$ reactions with large cross sections in low momentum transfer ($q < 100$ MeV/c) reaction such as the (K^-, π^-) reaction below 1 GeV/c. On the other hand, the ground state is produced by $\Delta L = 1$ reaction which requires a larger momentum transfer.

Previously, the weak decay of ${}^5_{\Lambda}\text{He}$ hypernucleus was studied twice, by employing the (K^-, π^-) reaction [7] and then by the (π^+, K^+) reaction [16, 9, 8]. As shown in Fig. 5, the (π^+, K^+) reaction spectrum shows a clearer ${}^6\text{Li}$ ground state peak. One reason is that the (π^+, K^+) reaction with a momentum transfer of $q \sim 350$ MeV/c has a significant cross section for the ${}^6\text{Li}$ ground state ($\Delta L = 1$) but almost no cross section for the substitutional states, although the non-substitutional $n(p_{3/2}^{-1})\Lambda(p_{3/2,1/2})$ states are also produced by $\Delta L = 2$ with some production cross sections. The other reason is that the (K^-, π^-) reaction suffers from a huge background from the decay of K^- beams into $\pi^-\pi^0$.

Therefore, in the proposed experiment we employ the (π^+, K^+) reaction at a beam momentum of 1.05 GeV/c, where the cross section for the $K^- n \rightarrow \Lambda \pi^-$ reaction is maximum. This reaction is the same as the one used in the previous ${}^5_{\Lambda}\text{He}$ weak decay experiment at KEK [16, 9, 8]. Although the cross section for ${}^6\text{Li}(\pi^+, K^+){}^6_{\Lambda}\text{Li}(\text{gs})$ was not measured, the yield of this reaction at 1.05 GeV/c was measured at KEK by using the same apparatus (the SKS septrometer) as the proposed experiment at J-PARC. Thus, the expected yield of the proposed experiment can be reliably estimated.

3 Measurement of the branching ratio

We determine the branching ratio of the beta-decay by measuring the beta-ray electron energy distributing from 0 to 163 MeV.

The weak decay of ${}^5_{\Lambda}\text{He}$ was previously studied at BNL via the (K^-, π^-) reaction and then at KEK via the (π^+, K^+) reaction. The lifetime of ${}^5_{\Lambda}\text{He}$ was measured to be 256 ± 21 ps [7] and 278^{+11}_{-10} ps [8], at BNL and KEK, respectively. It is almost the same as the lifetime of a free Λ of 263.2 ± 2.0 ps. The partial widths of the ${}^5_{\Lambda}\text{He}$ weak decay were also obtained in the KEK experiment as shown in Table 1.

3.1 Setup

The experiment will be carried out at the K1.1 beam line of the J-PARC Hadron Experimental Facility. The K1.1 beam line will be constructed and used for the E63 experiment near future.

Figure 6 shows the layout of the experimental setup. The momentum of each π^+ beam particle is analyzed by the K1.1 beamline spectrometer, and the scattered K^+ from the ${}^6\text{Li}$ target is identified and momentum analyzed by employing the Superconducting Kaon Spectrometer (SKS) [18]. The production of ${}^5_{\Lambda}\text{He}$ is identified from the missing mass of the ${}^6\text{Li}(\pi^+, K^+)$ reaction.

The beta-decay electron is measured by a newly-developed detector system around the target. It is identified by plastic hodoscope counters (TH) and Lucite Cherenkov counters (TLC) surrounding the target, and its total energy is measured by a BGO calorimeter (BGOC).

3.1.1 K1.1 beam line

The K1.1 beam line delivers separated beams up to 1.2 GeV/c, employing double-stage electrostatic separators (ESS1, ESS2) together with an intermediate focus point (IF). The π^+ beam intensity more than 3×10^7 /spill will be delivered for 30 MW operation, but the available beam intensity is limited by the counting rates of the tracking detectors installed upstream of the K1.1 spectrometer magnet. According to our experience in the E40 experiment at K1.8 beam line, the intensity of 3×10^7 /spill can be handled by employing a scintillating fiber tracking detector. A simulation using the Decay Turtle code shows that the beam size at the focusing point is smaller than ± 2 cm for horizontal and vertical directions.

3.1.2 K1.1 beam line spectrometer

At the K1.1 beam line, the last bending magnet (D4) together with Q10 and Q11 plays a role of the beam spectrometer. We employ the detectors which will be installed and used for the E63 experiment. At the entrance of D4 we install a tracking detector (BFT-U) made of 1 mm ϕ scintillating fibers arranged in 2 layers (0.5 mm pitch) and read out by MPPCs. It has a time resolution less than 2 ns (FWHM), providing a powerful means to select a true track when multiple beam tracks are recorded. We successfully used the same detector for J-PARC E10, E27 and E13 at the K1.8 beam line. It was confirmed at K1.8 that this detector can accept intense beam up to 3×10^7 /spill (2 s). At the exit of the beam line, we install two tracking detectors, one is a 1 mm-pitch MWPC (BC3) which was used at the upstream of the beam line spectrometer at K1.8 for the E19 and E10 experiments, and the other is a newly produced fiber tracking detector (BFT-D2) having the same configuration as BFT-U.

We install plastic scintillator hodoscopes (BH1, BH2) with 5 mm thickness having a timing resolution of <100 ps (FWHM) each. Protons and K^+ 's in the π^+ beam are easily rejected by time-of-flight.

The beam track is reconstructed from the hit point at BFT-U and those at BC3 and BFT-D2. The momentum resolution of the K1.1 beam line spectrometer is estimated to be 0.042% (FWHM) according to the simulation, giving a negligible effect to the energy resolution of the hypernuclear mass spectrum with our thick target of 14 g/cm².

The pion beam is irradiated on a 90%-enriched ⁶Li metal target with cylindrical shape of 4 cm in diameter and 30 cm in length (14 g/cm²).

3.1.3 SKS spectrometer

The scattered kaons are identified and momentum-analyzed by use of the SKS magnet, a scintillating fiber tracker (SFT) and drift chambers (SDC2,3,4), time-of-flight stop counters (TOF), aerogel Cherenkov counters (AC), and Lucite Cherenkov counters (LC). The setup is almost the same as that of the J-PARC E10 experiment for neutron-rich hypernuclear study via the (π^-, K^+) reaction [19, 20]. The geometrical setting of the SKS magnet will be changed back to the original one used in KEK E468 with a 100° bending angle for the central track. This setting will be also used for the E63 and other proposed experiments at K1.1.

The SKS spectrometer sustains an acceptance of about 100 msr at maximum and covers a wide range of scattering angle ($15^\circ < \theta < 15^\circ$). It covers almost all the scattering angles for $^5_\Lambda\text{He}$ production having a forward ($\theta = 0^\circ$) cross section peak with a width of $\pm 10^\circ$ (FWHM).

We expect to have a hypernuclear mass resolution of ~ 2.0 MeV (FWHM) without energy loss effect in the target. Thus, the actual mass resolution will be determined by energy loss effect in the 14 g/cm²-thick ⁶Li target. It is estimated to be ~ 4 MeV (FWHM). Actually, the mass resolution

of 4.2 MeV (FWHM) was achieved in KEK E419 experiment using the same SKS setup and a 13.7 g/cm²-thick ⁷Li metal target [21]. The expected resolution is sufficient to observe the ⁶ΛLi(gs) peak. In the experiment we also take a spectrum with a thin ⁶Li target, which will be convoluted with a response function of ~4 MeV (FWHM) width and used to decompose the thick target spectrum to extract the ⁶ΛLi(gs) events precisely.

3.1.4 Counters surrounding the target

Figure 7 shows a schematic view of the setup around the target. The target is 90%-enriched ⁶Li metal with a cylindrical shape with a 4 cm diameter and a 14 g/cm² (30 cm) length packed in a laminated plastic bag filled with Ar gas. The shaped and packed ⁶Li target is available from a company in Japan.

The cylindrical target is surrounded by circumferentially segmented plastic counters (TH, Target Hodoscope) of 50 cm long along the beam direction. It has a thickness of 5 mm and a width of ~4 mm. They measure the timing, the multiplicity, the energy loss, and the hit position of the charged particle(s). The signal of each plastic counter is read out via MPPC's attached at both ends, and their timing difference is converted to the hit position along the beam direction. The position resolution along the beam direction is assumed to be 20 mm (rms) in the following simulation.

The target and TH are surrounded by circumferentially segmented Lucite Cherenkov counters (TLC, Target Lucite Cherenkov) with the index $n \sim 1.5$ to discriminate electrons ($\beta = 1$) from weak decay pions ($\beta < 0.610$ for $p_\pi < 140$ MeV/c in a nucleus) and protons. Each TLC counter, of which dimensions are 5 mm thick, 8mm wide and 50 cm long, is read out with MPPC's at both ends. We expect that the TLC efficiency for electron is more than 99%, but the misidentification rate for charged pions and protons due to δ -rays is considered to be 4% according to a simulation.

The target area is surrounded by a BGO calorimeter (BGO) which measures electron energies up to 200 MeV. Optimization and detailed design of the BGO is on going. In the following simulation, BGO is assumed to have a thickness of 20 cm (18 radiation length) with the inner radius (distance for the center to the surface of the BGO) of 30 cm, and segmented into 225 crystal pieces. Each crystal has a size of about 7 cm \times 7 cm \times 20 cm. The GEANT4 geometry of the setup around the target is shown in Fig. 8.

Since the counting rate for the BGO counters located around the downstream hole is expected to be higher than the operation limit, even if the pulse shape of each BGO counter is recorded and pile-up signals are decomposed in off-line analysis. After careful estimation of the counting rates, we will need to change a part of the BGO counters into faster scintillation counters, or, into photon veto counters such as leadglass Cherenkov counters or plastic+lead counters.

3.2 Background suppression

This measurement suffers from the following background processes. We have studied how to suppress them via simulations by using the GEANT4 code.

(1) π^0 from $\Lambda \rightarrow n\pi^0$

Most of this type of background events can be rejected by requiring hits in TH and in TLC and a single cluster hit in BGO. Figure 9 shows the number of hit clusters in BGO for the beta-decay electron and the mesonic decay π^- and π^0 from Λ , calculated in the simulation. By selecting single cluster events, about 97% of the π^0 events are rejected. In most of the remaining events, one

of the two photons from π^0 escapes from the upstream or downstream holes of BGOC. (The size of 30 msr for the upstream hole and 90 msr for the downstream hole in the present simulation.)

Since a photon from π^0 is converted to an e^-e^+ pair in the target or in TH in $\sim 4\%$ probability, $3\% \times 4\% = 0.12\%$ of π^0 events cannot be rejected. By multiplying the π^0 decay branching ratio of 0.20 (Table 1), this contamination has a branching ratio of 0.024%. In order to suppress those events further, we request the pulse height of TH to be consistent with one minimum-ionizing particle passing through the detector so that we can reject events of pair creation in the target for which the TH pulse height is twice larger. As shown in Fig. 10, our simulation showed that this method suppresses those remaining π^0 events by 1/4 after taking into account the path length in the target calculated from the BGOC hit point and the reaction vertex point. In addition, even if a photon is not converted around the target and does not give a pulse in TH and TLC, it produces an electromagnetic shower in BGOC from which an e^- or e^+ can be emitted back to the target region and hit TH and TLC. Such events can be suppressed by investigating correlation of the reaction vertex point in the target, the cluster position in BGOC, and the hit position in TH.

According to the simulation, the analysis described above suppresses the π^0 background down to the branching ratio of 0.007%, which corresponds to 8% of the beta-decay events. On the other hand, the number of true beta-decay events is also reduced by those cuts through the whole analysis. The beta-ray analysis efficiency was found to be 68%. Namely, the background/signal ratio is 12%.

In order to further reduce the background by detecting a photon which escapes from the downstream hole of BGOC, we will install photon veto counters around the entrance of the SKS magnet and on the surface of the pole face and the side wall of the SKS magnet. We expect such detectors will reduce the background by a factor of two or more.

Thus we will be able to suppress the π^0 background down to the branching ratio of 0.0035% (the background/signal ratio is 6%).

(2) π^- from $\Lambda \rightarrow p\pi^-$

π^- mesons emitted from the target are discriminated from electrons by use of TH pulse height and the number of hit clusters in BGOC. Since the pion momentum from the Λ hypernuclear weak decay distributes around 100 MeV/c and the maximum momentum is around 140 MeV/c, such pions do not emit Cherenkov light in Lucite but in a few per cent probability (in 4.5% in the present simulation) a δ -ray is emitted in TH, misidentifying the pion as an electron. Further suppression of π^- can be done from the number of clusters in BGOC, because such a low-momentum π^- is absorbed by a nucleus in BGO, before or after stopping, via the $\pi^- + pn \rightarrow n + n$ reaction in most cases. These two neutrons make the number of the BGOC clusters larger than 1. As shown in Fig.9, the fraction of one cluster events is 23%. In addition, by requiring the number of hit segments in BGOC, the π^- background is further suppressed, and the remaining π^- background is found to have a branching ratio of 0.19%.

Here, by applying the same cuts as used for the π^0 background suppression, the π^- background can be further suppressed. In particular, since dE/dx of π^- is almost twice larger than that of the beta-ray electron, TH pulse height cut after correcting for the path length is very effective. We found that the π^- background is finally reduced to a branching ratio of 0.0004%, which corresponds to the background/signal ratio of only 0.16%.

Table 2: Expected yield of the ${}^5_{\Lambda}\text{He}$ hypernuclei and its beta decay events estimated in comparison with the ${}^5_{\Lambda}\text{He}$ yielded measured in KEK E462 experiment.

Experiment	E462	Proposed experiment
Number of π^+ beam	2.5×10^{12}	43×10^{12}
${}^6\text{Li}$ target thickness	3.70 g/cm ² (80 mm)	14 g/cm ² (300 mm)
${}^5_{\Lambda}\text{He}$ counts after SKS analysis	45653	2.0×10^6
BR_{β}		8×10^{-4}
Pauli suppression effect		0.6
e^- detection efficiency		0.7
Beta-ray counts		673

(3) Protons and neutrons from nonmesonic weak decay

A proton from nonmesonic weak decay, $\Lambda p \rightarrow np$, has an energy of ~ 80 MeV ($\beta \sim 0.41$) at maximum. It does not emit Cherenkov light in TLC and the energy loss in TH is more than 4 times larger than that for electrons. Neutrons from nonmesonic weak decay, $\Lambda p \rightarrow np$ and $\Lambda n \rightarrow nn$, also have energies of 80 MeV or lower. A simulation showed that these processes are suppressed to less than 10^{-5} by the same cut analysis as used in (1) and (2).

3.3 Yield and accuracy of the branching ratio

In order to measure the beta-decay branching ratio within a statistical error of 4%, we need to collect more than $(1/0.04)^2 = 625$ counts of the beta-decay events. To estimate the yield of ${}^5_{\Lambda}\text{He}$ hypernuclei, we refer to the KEK E462 experiment. This experiment irradiated 2.5×10^{12} π^+ on a 3.70 g/cm²-thick ${}^6\text{Li}$ metal target and obtained 45653 counts of ${}^5_{\Lambda}\text{He}$ events employing the SKS spectrometer. Since the geometrical setup of the SKS spectrometer including detectors is identical, we can estimate the yield of ${}^5_{\Lambda}\text{He}$ in our experiment as shown in Table 2.

The beta-decay rate is reduced due to Pauli effect because the proton from $\Lambda \rightarrow pe^- \bar{\nu}$ has a recoil momentum between 0 to 163 MeV/c, lower than the Fermi momentum. As shown in Table 1, the mesonic decay rate is reduced as $(\Gamma_{\pi^-} + \Gamma_{\pi^0})/\Gamma_{\Lambda} = 0.54$ in ${}^5_{\Lambda}\text{He}$ due to Pauli effect of a proton of ~ 100 MeV/c and the pion absorption effect. Thus we assumed the Pauli suppression factor for the beta-decay proton as 0.6. This value will be theoretically estimated later.

The efficiency for beta-ray electron detection, which includes various cuts in the background suppression analysis as well as the BGOC acceptance (99%), is assumed to be 0.7. The number of beta-decay events for $43 \times 10^{12} \pi^+$ beams is calculated to be 673 counts. This number of π^+ beams corresponds to 1400 hours for the beam intensity of $30 \times 10^6 \pi^+$ per spill for 5.2 s operation cycle. Thus, a statistical error less than 4% is achieved in the beam time of 1400 hours.

According to the simulation, all the background processes shown above will be sufficiently suppressed. Figure 11 shows a simulated final spectrum of single electrons (beta-ray) after applying all the background suppression analysis. The yield of the beta-ray is reduced to 68%, while 99.994% of π^0 background events and 99.999% of the π^- background events are rejected. The fraction of the remaining background events is 4% of the beta-ray events, as shown in red in Fig. 11.

Since the rejection efficiency for each background process can be estimated by realistic simulations, the number of remaining background events in the final spectrum can be estimated and

subtracted. Even if the rejection efficiency is estimated in 25% uncertainty, the systematic error of the beta-ray counts coming from the background will be 1%, being much lower than the expected statistical error of 4%.

It is to be noted that the $\Lambda \rightarrow n\gamma$ decay will be also clearly observed as a peak in the photon spectrum in the same dataset and its branching ratio will be also determined.

4 Measurement of the lifetime

Employing a setup slightly modified from the branching ratio measurement, the lifetime of ${}^5_{\Lambda}\text{He}$ is measured in the same ${}^6\text{Li}(\pi^+, K^+){}^6\text{Li}(\text{gs})$ reaction as the time difference between the beam π^+ timing and the emission timing of the weak decay particles. Here, as the decay particles, we use energetic protons ($\sim 30\text{--}80$ MeV) from nonmesonic weak decay ($\Lambda p \rightarrow pn$) of ${}^5_{\Lambda}\text{He}$, because those protons provide a large pulse in the timing counter, making the time resolution better than other particles. It is the same method as the ${}^5_{\Lambda}\text{He}$ lifetime measurement in KEK E462.

The timing of the beam pion and that of the decay proton emitted around the target are measured with fast-timing plastic counters, T1 and T2, respectively. The time difference between them is plotted as a “decay time spectrum” after correcting for the π^+ flight time from the beam counter (T1) to the reaction point, as well as the proton flight time from the reaction point to the decay counter (T2). Here, the beam and the proton trajectories as well as the proton energy should be also measured. In addition, the decay time spectrum for the prompt reaction, ${}^6\text{Li}(\pi^+, pp)$, in which one proton is detected by SKS and another proton by T2, will be also measured and used as a response function when fitting the decay time spectrum of ${}^5_{\Lambda}\text{He}$.

The previous experiment, KEK E462, was successfully conducted by this method. Figure 12 shows the decay time spectra for ${}^5_{\Lambda}\text{He}$ and ${}^{12}_{\Lambda}\text{C}$ hypernuclei measured in E462. This experiment achieved lifetime precision of 4% for ${}^5_{\Lambda}\text{He}$ and 3% for ${}^{12}_{\Lambda}\text{C}$, which was limited by statistics due to negligible systematic errors [17]. In the proposed experiment, we will take data with four times higher statistics and with the same or better time resolution to achieve 2% accuracy.

4.1 Setup

The lifetime of ${}^5_{\Lambda}\text{He}$ is measured separately from the branching ratio measurement using the modified setup around the target optimized for the precise lifetime measurement.

Figure 13 shows a top view of the detectors around the target. We install a plate of ${}^6\text{Li}$ metal target, and fast timing counters with a time resolution of < 50 ps rms just upstream of the target (T1) and at the left and right sides of the target (T2L, T2R). The target is a 90%-enriched ${}^6\text{Li}$ metal plate of 30 mm in thickness and 100 mm in length. T1 is made of 20 pieces of 2 mm-wide 50 mm-long 5 mm-thick plastic counter, each of which is read out via MPPC at both ends. T2L and T2R are made of 20 pieces of 4 mm-wide 150 mm-long 5 mm-thick plastic counter, each of which is read out via MPPC’s at both ends. In order to measure the position of the proton in the beam direction, we also install plastic hodoscopes, THL and THR, outside of T2L and T2R. Each of them is made of 80 pieces 3 mm-thick plastic counters of 2 mm wide and 80 mm long, read out via MPPC’s from one end.

4.2 Yield and accuracy of the lifetime

The yield of the nonmesonic proton events of ${}^5_{\Lambda}\text{He}$ is estimated based on the KEK E462 results as shown in Table 3. By irradiating the same number of π^+ as E462 (2.5×10^{12}), which corresponds

Table 3: Expected yields of the ${}^5_{\Lambda}\text{He}$ hypernuclei and their nonmesonic proton events, and then the expected lifetime accuracy, are estimated in comparison with the KEK E462 results.

Experiment	E462	Proposed experiment
Number of π^+ beam	2.5×10^{12}	2.5×10^{12}
${}^6\text{Li}$ target thickness	3.70 g/cm ² (80 mm)	4.6 g/cm ² (100 mm)
${}^5_{\Lambda}\text{He}$ counts after SKS analysis	45653	5.7×10^4
BR_p [16]	0.28	0.28
proton detection efficiency		0.3
Proton counts	~ 1030	4768
Time resolution (rms)	128 ps	128 ps
Statistical error of lifetime	4.0%	1.9%

to 120 hours of beam time for $3 \times 10^7 \pi^+/\text{spill}$, we will be able to collect nonmesonic proton events of more than 4 times, which leads to twice better statistical accuracy (a relative error of 2%).

5 Cost, Schedule, Man power

After the K1.1 beam line is built and the E63 experiment is conducted, almost all the apparatus and the detectors for the K1.1 spectrometer and the SKS spectrometer are available. However, the apparatus around the target should be carefully designed and fabricated. In particular, the geometry and segmentation of BGO-C will be optimized based on more realistic simulations. In addition, detailed simulation studies for background suppression with the realistic setup will be carried out.

The total detector cost will be 200-400 M yen, and more than a half will be used for BGO-C. A Kakenhi grant will be requested soon and other financial sources will be searched for.

The design work and detector R&D/fabrication will be carried out mainly by Tohoku University group in collaboration with JAEA and KEK people. We will soon start organizing collaborators including oversea scientists. The preparation will take at least 4 years. We hope to run this experiment at the K1.1 beam line, hopefully in the extended Hadron Experimental Facility, in 5-6 years.

References

- [1] D. F. Geesaman, K. Saito, A. W. Thomas, Ann. Rev. Nucl. Part. Sci. 45 (1995) 337.
- [2] L. B. Weinstein et al., Phys. Rev. Lett. 106 (2011) 052301.
- [3] P. A. M. Guichon, A.W. Thomas, Phys. Lett. B773 (2017) 332.
- [4] W. T. Chou et al., Phys. Rev. C 47 (1993) 163.
- [5] F. C. Khanna, I. S. Towner, H. C. Lee, Nucl. Phys. A 305 (1978) 349.
- [6] S. Vaintraub, N. Barnea, D. Gazit, Phys. Rev. C79 (2009) 065501.

- [7] J.J. Szymanski et al., Phys. Rev. C43 (1991) 849.
- [8] S. Kameoka et al., Nucl. Phys. A754 (2005) 173c.
- [9] S. Okada et al., Phys. Lett. B 597 (2004) 249; S. Okada et al., Nucl. Phys. A754 (2005) 178c.
- [10] T. Motoba, H. Bandō, T. Fukuda, J. Žofka, Nucl. Phys. A534 (1991) 597.
- [11] I. Kumagai-Fuse, S. Okabe, Y. Akaishi, Phys. Rev. C 54 (1996) 2843.
- [12] K. Itonaga, T. Motoba, Prog. Theor. Phys. Suppl. 185 (2010) 252.
- [13] A. Parreno, A. Ramos, Phys. Rev. C 65 (2001) 015204.
- [14] C. Barbero, C. De Conti, A.P. Galeao, F. Krmpotic, Nucl. Phys. A 726 (2003) 267.
- [15] R. Bertini et al., Nucl. Phys. A368 (1981) 365.
- [16] B.H. Kang et al., Phys. Rev. Lett. 96 (2006) 062301.
- [17] S. Kameoka, Ph.D thesis, Tohoku University (2005).
- [18] T. Takahashi et al., Prog. Theor. Exp. Phys. 2012 (2012) 02B010.
- [19] H. Sugimura et al., Phys. Lett. B 729 (2014) 39.
- [20] R. Honda et al., Phys. Rev. C 96 (2017) 014005.
- [21] H. Tamura et al., Phys. Rev. Lett. 84 (2000) 5963.

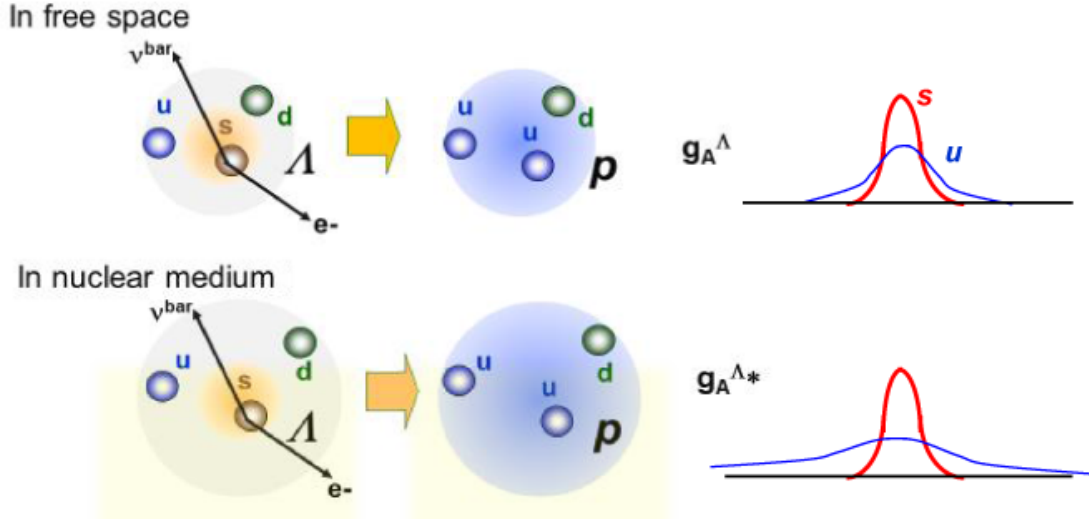


Figure 1: Illustration for possible modification of spatial distribution of quarks in nuclear matter and its effect to beta decays. Distribution of u and d quarks are expected to be more spread in a nucleus but that os s quarks are less spread. Thus the overlap between the s and u quark wave functions in the hyperon beta decay is expected to be decreased..

Reaction	$2J_k^{\pi}, 2T$		$\log f_{At}$	$M(GT)$ (exp)	$M(GT)$ th(free)	g_A^{exp} / g_A
	(i)	(f)				$\frac{M(GT)_{exp}}{M(GT)_{th(free)}}$
${}^1_0\text{n}(\beta^-){}^1_0\text{H}$	$1^+, 1$	$1^+_1, 1$	3.024(1)	3.100(7)	3.096	1.00
${}^3_0\text{H}(\beta^-){}^3_0\text{He}$	$1^+, 1$	$1^+_1, 1$	3.058(1)	2.929(5)	3.096	0.946
${}^6_0\text{He}(\beta^-){}^6_0\text{Li}$	$0^+, 2$	$2^+_1, 0$	2.910(1)	2.748(4)	3.031	0.907
${}^7_0\text{Be}(EC){}^7_0\text{Li}$	$3^-, 1$	$3^-_1, 1$	3.300(1)	2.882(4)	3.187	0.904
${}^{11}_0\text{C}(\beta^+){}^{11}_0\text{B}$	$3^-, 1$	$3^-_1, 1$	3.598(2)	1.480(9)	2.084	0.710
${}^{13}_0\text{N}(\beta^+){}^{13}_0\text{C}$	$1^-, 1$	$1^-_1, 1$	3.671(2)	0.788(8)	0.891	0.884

Figure 2: Experimentally measured beta-decay rates in terms of the $\log f_{At}$ values and Gamow-Teller transition matrix elements ($M(GT)$) for light nuclei [4]. Measured $M(GT)$ values normalized by theoretical $M(GT)$ values corresponds to the g_A quenching factor of g_A^{exp} / g_A as shown in red.

Λ DECAY MODES	Fraction (Γ_i/Γ)	Confidence level (ρ) (MeV/c)
$p\pi^-$	$(63.9 \pm 0.5) \%$	101
$n\pi^0$	$(35.8 \pm 0.5) \%$	104
$n\gamma$	$(1.75 \pm 0.15) \times 10^{-3}$	162
$p\pi^- \gamma$	[c] $(8.4 \pm 1.4) \times 10^{-4}$	101
$pe^- \bar{\nu}_e$	$(8.32 \pm 0.14) \times 10^{-4}$	163
$p\mu^- \bar{\nu}_\mu$	$(1.57 \pm 0.35) \times 10^{-4}$	131

$pe^- \bar{\nu}_e \quad g_A/g_V = -0.718 \pm 0.015$ [b]

Figure 3: Decay branching ratio of Λ from Particle Data Book.

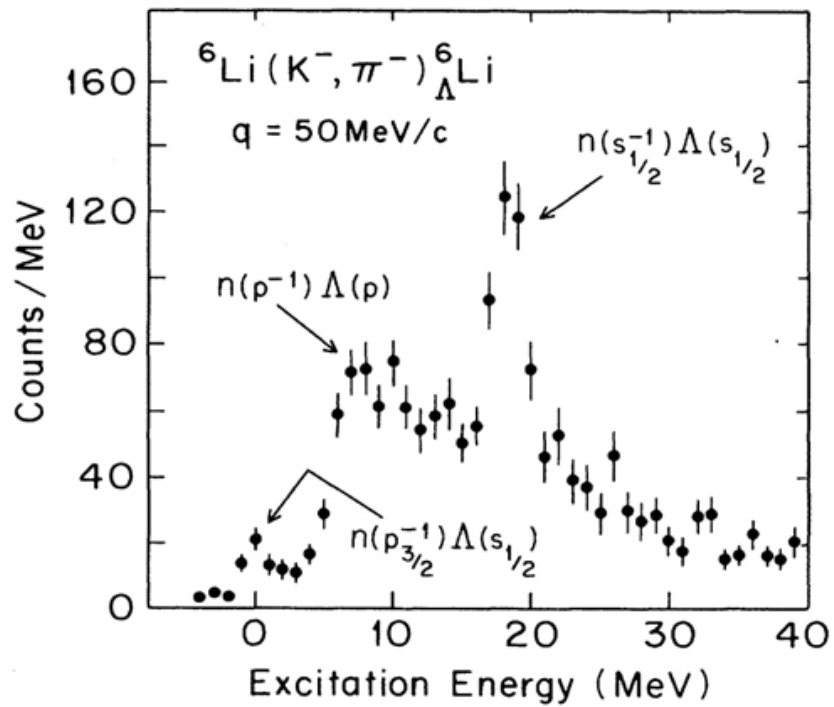


Figure 4: Excitation energy spectrum of ${}^6\text{Li}$ produced by the (K^-, π^-) reaction [15]. The ${}^6_\Lambda\text{Li}$ ground state peak is clearly seen.

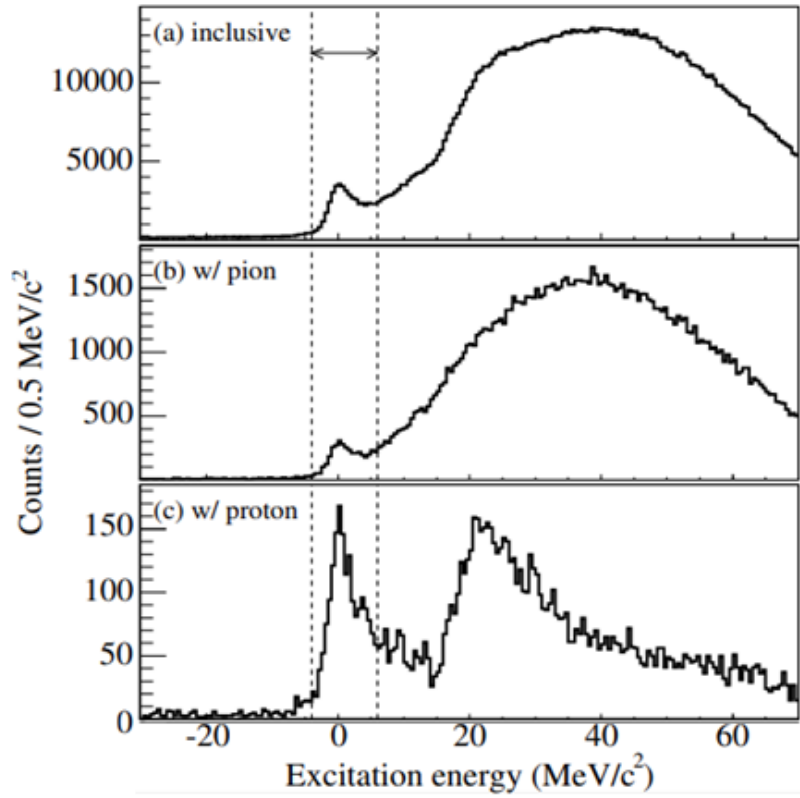


Figure 5: Excitation energy spectrum of ${}^6\text{Li}$ produced by the (π^+, K^+) reaction [17]. (b) and (c) show the spectra in coincidence with pions and protons. The ${}^6_\Lambda\text{Li}$ ground state peak is clearly seen in any of the coincidence spectra.

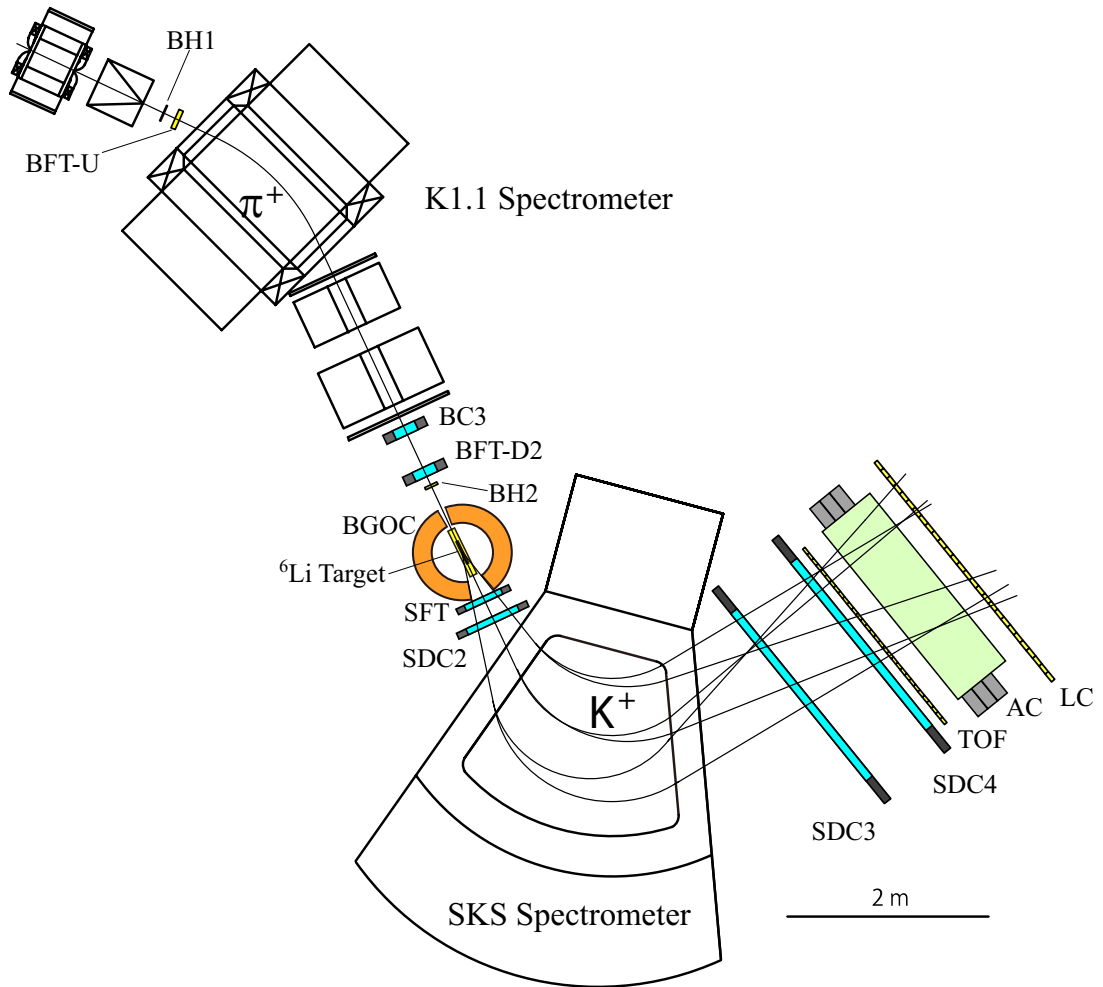


Figure 6: Setup of the experiment at K1.1 beam line.

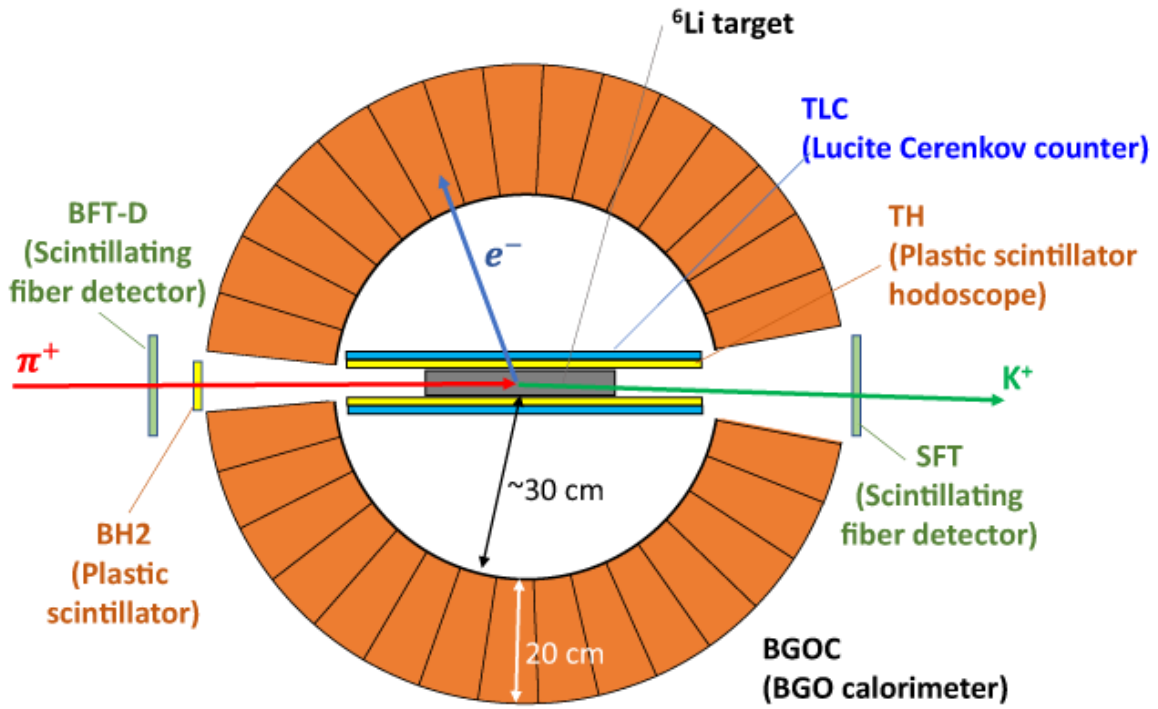


Figure 7: Setup around the target for the branching ratio measurement.

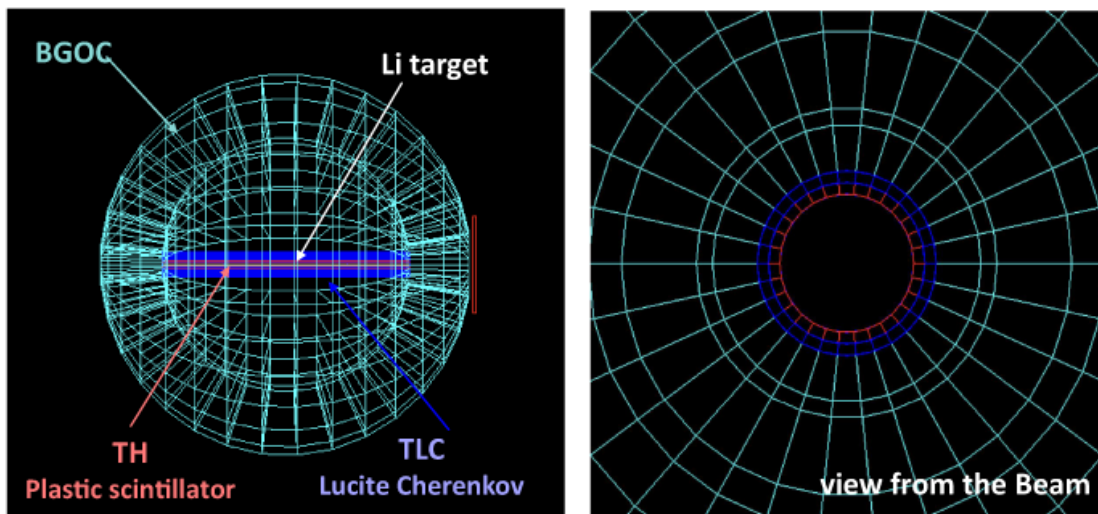


Figure 8: GEANT4 geometry of the setup around the target used in the present simulation.

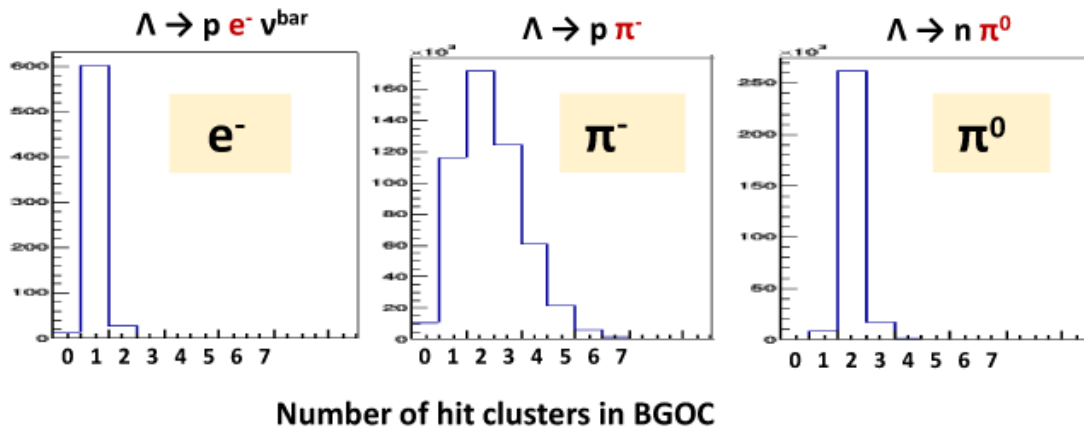


Figure 9: Simulated number of hit clusters in BGOC for beta-decay electron, mesonic decay π^- , and mesonic decay π^0 of Λ weak decay.

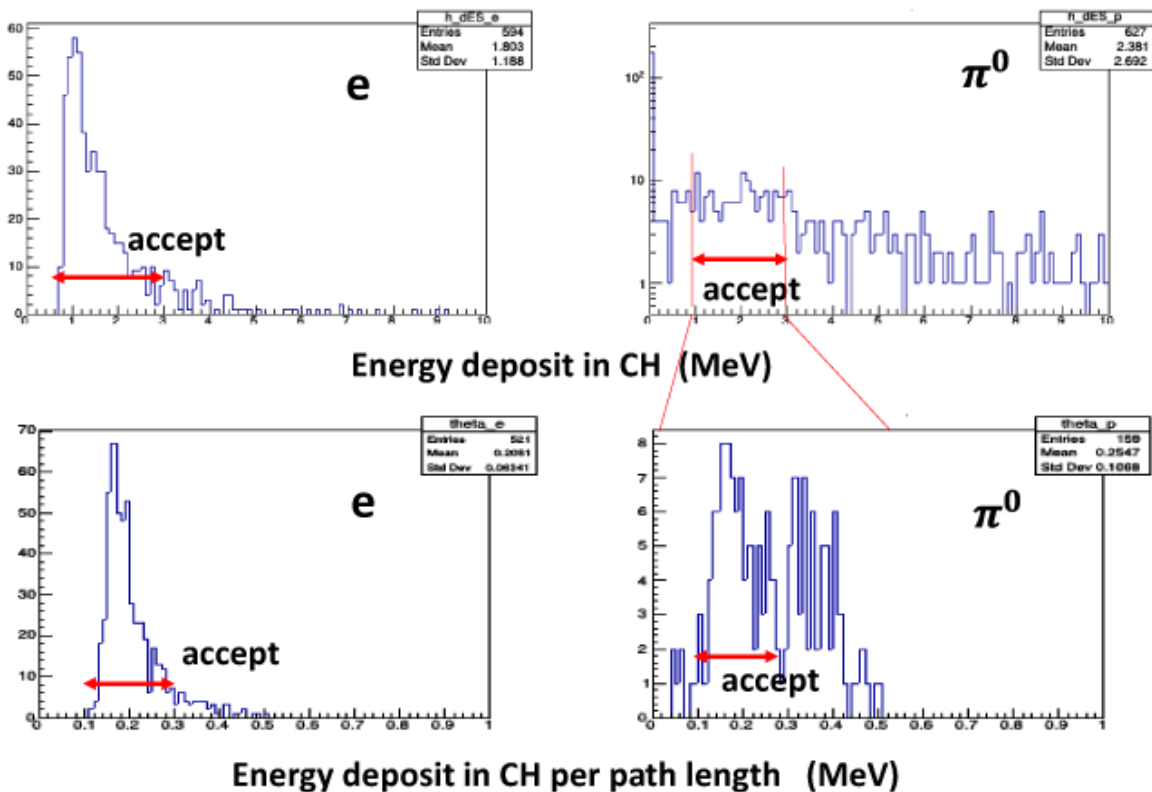


Figure 10: Simulated energy deposit in TH for the beta-decay electron event (left), and for the mesonic decay π^0 event in which one of the two photons is converted to e^-e^+ pair in the target region (right). The lower figures show the same energy deposit but normalized for the path length in the TH counter.

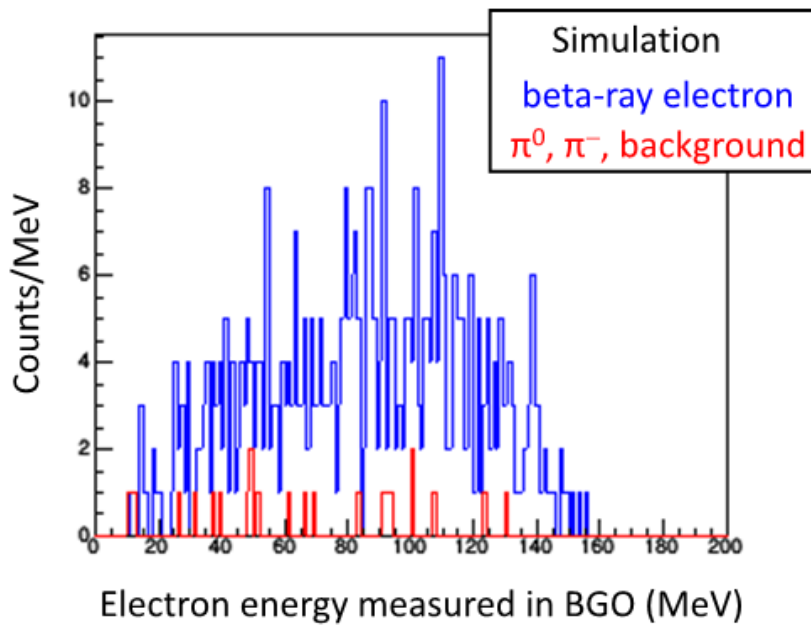


Figure 11: Simulated spectrum of the beta-ray electron energy (blue) and the contaminated background events (red) after all the background rejection analysis. The number of the background events is 4% of that of the beta-ray electron.

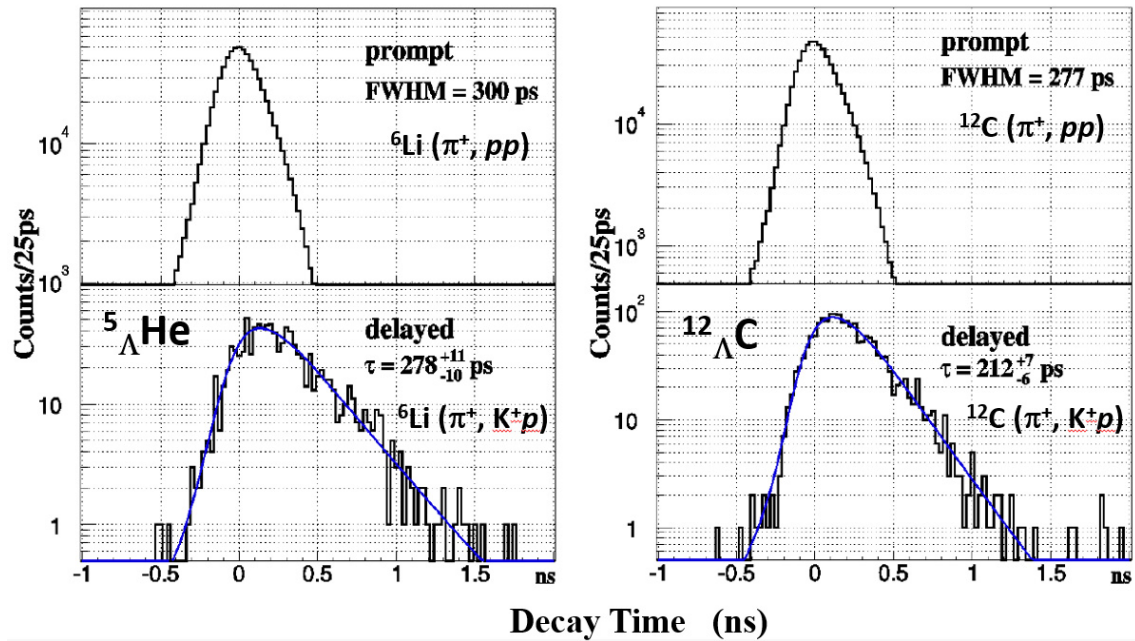


Figure 12: Decay time spectra for ${}^5_{\Lambda}\text{He}$ and ${}^{12}_{\Lambda}\text{C}$ measured in KEK E462 experiment. The upper panels show “response function” of the spectrum measured with the prompt reaction of (π^+, pp) , while the lower panels show decay time spectra for ${}^5_{\Lambda}\text{He}$ and ${}^{12}_{\Lambda}\text{C}$ hypernuclei via (π^+, K^+p) reaction.

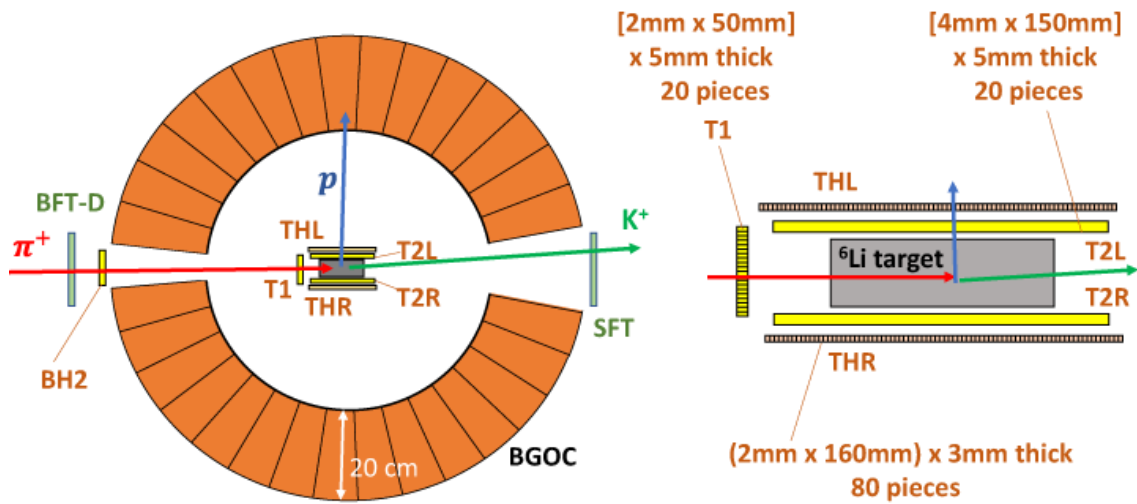


Figure 13: Schematic view of the setup around the target for the lifetime measurement.